Neural Activity in Primary Motor Cortex Related to Mechanical Loads Applied to the Shoulder and Elbow During a Postural Task

D. WILLIAM CABEL,[1] PAUL CISEK,[2] AND STEPHEN H. SCOTT[1]
[1]Canadian Institutes of Health Research Group in Sensory-Motor Systems, Department of Anatomy and Cell Biology, Queen's University, Kingston, Ontario K7L 3N6; and [2]Départment de physiologie, Université de Montréal, Montreal, Quebec H3C 3J7, Canada

Cabel, D. William, Paul Cisek, and Stephen H. Scott. Neural activity in primary motor cortex related to mechanical loads applied to the shoulder and elbow during a postural task. *J Neurophysiol* 86: 2102–2108, 2001. Whole-arm motor tasks performed by nonhuman primates have become a popular paradigm to examine neural activity during motor action, but such studies have traditionally related cell discharge to hand-based variables. We have developed a new robotic device that allows the mechanics of the shoulder and elbow joints to be manipulated independently. This device was used in the present study to examine neural activity in primary motor cortex (MI) in monkeys (*macaca mulatta*) actively maintaining their hand at a central target as they compensated for loads applied to the shoulder and/or elbow. Roughly equal numbers of neurons were sensitive to mechanical loads only at the shoulder, only at the elbow, or loads at both joints. Neurons possessed two important properties. First, cell activity during multi-joint loads could be predicted from its activity during single-joint loads as a vector sum in a space defined by orthogonal axes for the shoulder and elbow. Second, most neurons were related to flexor torque at one joint coupled with extensor torque at the other, a distribution that paralleled the observed activity of forelimb muscles. These results illustrate that while MI activity may be described by independent axes representing each mechanical degree-of-freedom, neural activity is also strongly influenced by the specific motor patterns used to perform a given task.

INTRODUCTION

Primary motor cortex is known to be intimately involved in volitional motor control, yet little is known on how this region coordinates motor patterns at different joints (Drew et al. 1996; Murphy et al. 1985; Scott 2000). Although few would doubt that the activity across primary motor cortex (MI) is involved in controlling the whole limb, the crucial question is how individual neurons participate in this process. Many studies have examined neural activity during whole-arm motor tasks in monkeys (Georgopoulos 1995; Kalaska et al. 1997), but for technical reasons, these studies have correlated neural activity to variables related to the hand. Although neural activity has been shown to be broadly tuned to the direction of hand movement, several studies illustrate that other factors related to the motor periphery often influence cell discharge (Kalaska et al. 1989; Scott and Kalaska 1997; see also Kakei et al. 1999). Since these motor tasks only consider hand-based variables,

inferences on how the neural activity may be related to the underlying mechanics at the shoulder and elbow cannot be explored.

We have recently developed a new experimental device that can directly manipulate the mechanics of the shoulder and elbow joints of monkeys (Scott 1999). This device allows us to examine whole-limb motor tasks where the global goal is to move or maintain the hand in space while systematically modifying the properties of each joint independently. The present study illustrates the first description of the response of motor cortical neurons using this device. Monkeys were trained to maintain their hands at a central target while flexor or extensor loads were applied to the shoulder and/or elbow joints. The experimental data illustrate specific features on how neural discharge reflects the mechanical loads at multiple joints.

METHODS

Three juvenile male rhesus monkeys each weighing approximately 7 kg were used in this study, two for the neural recordings and all three for the electromyographic recordings. Each monkey was trained to wear a mechanical exoskeleton on its right arm that permitted flexion and extension motion of the shoulder and elbow joints in the horizontal plane (Scott 1999). Hinge joints on the device were aligned with the monkey's shoulder and elbow joints, and custom-made arm troughs attached the linkage to its upper arm and forearm. Motors attached to the linkage monitored joint angle and allowed mechanical loads to be applied to the shoulder and/or elbow joints. Each monkey was trained to maintain its right hand within an 8-mm radius target positioned in the center of the work-space. Constant-magnitude torques (± 0.11 Nm) were applied by the device to the shoulder and/or elbow joints. Three loads were used at each joint (flexor, null, and extensor), giving a total of nine load conditions for the two joints. A load applied to one joint required the monkey to change the net muscular torque only at that joint while maintaining the muscular torque at the other joint unchanged. The magnitude of the load was sufficiently large to require the monkey to actively control the position of the hand and create measureable changes in forelimb muscle and MI activity (see RESULTS) and was small enough that the monkeys would perform the task throughout a 2- to 3-h recording session. For each trial, the load was first applied, the target light was then illuminated, and the monkey was required to move to and maintain its hand at the central target for more than 3 seconds. The monkey was trained to maintain its hand on the surface of the forelimb/hand trough so that

---

Address for reprint requests: S. H. Scott, Dept. of Anatomy and Cell Biology, Queen's University, Kingston, Ontario K7L 3N6, Canada (E-mail: steve@biomed.queensu.ca).

the mechanical load was applied directly to the upper arm and forearm, and not through the hand. Five repeat trials of each load condition were presented in a pseudo-random block design. Data analyses were based on the mean discharge of the cell for the last 2 seconds of each trial.

We used conventional techniques for extracellular recording of single neuron activity related to the proximal arm in primary motor cortex (Scott and Kalaska 1997). Recording chambers were implanted surgically under inhalation anesthetic. Neurons recorded in the task were located in the rostral bank and crown of the central sulcus where trains of electrical stimulation (11 pulses, 333 Hz, 0.2-ms pulse width, range 5–50 μA) elicited movement of the shoulder or elbow. The territory where cell activity was sampled in motor cortex was similar to the region examined in previous studies on reaching (Scott and Kalaska 1997). Cells were examined in the task if they responded only to passive movement of the shoulder or elbow. Cells that did not respond to passive movement of any of the forelimb joints were recorded in the task if neighboring neurons responded to passive movement of the shoulder and elbow. Many of the neurons recorded in the present postural task were also active for other tasks, such as reaching. A full account of the response of these neurons both within and between tasks will be presented in future studies. All procedures were approved by the Queen's University Animal Care Committee and followed university and national guidelines for animal care.

Previous studies examining neural activity in motor cortex during multi-joint motor tasks have traditionally used experimental paradigms with movements or loads that are equally distributed in space and of similar magnitude (Georgopoulos et al. 1982; Kalaska et al. 1989; Scott and Kalaska 1997). The directional tuning of a cell can then be defined by scaling unit vectors aligned with the direction of movement (or load) by the discharge of the cell during each trial and then summing these vectors for each direction to provide the cell's directional preference. The purpose of the present article was to relate neural activity to loads applied at each individual joint so the loads were kept constant at each joint regardless of the load at the other joint. Therefore the magnitude of the total torque at the two joints was 0.22 Nm when loads were applied at both joints and 0.11 Nm when loads were applied at only one joint. To remove any possible effect that load magnitude may have on estimates of each cell's preferred direction (PD) in joint torque space, trials were divided into two groups: those where torques were applied at only one of the two joints and those where torques were applied concurrently at both joints. For each block of trials, a PD was calculated for each group by scaling unit vectors aligned with the direction of load in joint-torque space by the discharge of the cell during that trial and then summing these vectors for each load condition in that group. This created two PDs, one for each group, and these were averaged to identify a PD for each block of trials. A cell's PD was defined as the average from the five repeat blocks. Except for the division of trials into two groups, this technique is identical to that used in previous studies (Scott and Kalaska 1997). We compared the PD generated using the techniques described above as compared with the PD computed based on single-joint loads only or multi-joint loads only. The average absolute difference in the PD was only 8.8°, suggesting that the division of trials into two groups and then averaging the results had a minimal effect on the PD for each cell. The significance of the PD for each cell was determined using a "bootstrapping" statistical method (Scott and Kalaska 1997). This method compares the length of the PD vector "R" based on the cell's discharge during the task as compared with values of R based on random reshuffling of the discharge rates across all load conditions. The cell's discharge pattern was statistically tuned if fewer than 40 of 4,000 reshuffled samples (1%) had larger mean vector lengths than that observed in the task (unshuffled data).

A two-factor ANOVA was used to define whether a cell was modulated by loads at the shoulder and/or elbow joints. The ANOVA used elbow and shoulder muscular torque as factors with three levels within each factor: the requirement of an extensor, flexor, and un-loaded torque. ANOVA results flagged significant changes in cell discharge across the three levels of each factor and were used to classify cells as related to the shoulder, the elbow, or to both joints. Note that the two main statistical tests used in this study (ANOVA and directional preference) are not identical, and therefore the number of cells flagged by each test will not be identical (see RESULTS). For example, a cell that increased its activity both for flexor and extensor torques at the elbow and did not respond to the shoulder loads would be flagged as an "elbow" cell by the ANOVA, but would not be found to be directionally tuned.

The present experimental paradigm allows us to examine how the discharge patterns of MI cells reflect mechanical loads at multiple joints simultaneously. The response of each neuron for shoulder, elbow, and combined loads can be defined as Vectors (S, E, and ES, respectively). The length of Vector S was calculated as the absolute difference in cell discharge rate between flexor and extensor loads applied to the shoulder. The length of Vector E was defined in a similar manner for flexor and extensor loads at the elbow. The length of Vector ES was defined as the absolute difference in cell discharge rate between the multi-joint load closest to the cell's joint-torque PD and the opposite load. We tested two models to identify whether the activity of neurons during multi-joint loads could be predicted from their responses to single-joint loads. In essence, we tested whether Vector ES could be predicted from Vectors E and S. One possibility is that Vectors E and S are aligned and oriented in the same direction (left panel of Fig. 2A). In this Linear Summation Model, the activity of a cell when loads are applied to both joints equals its activity when a load is applied only at the shoulder added to its activity when a load is applied only at the elbow. A second possibility is that Vectors E and S are orthogonal to each other (left panel of Fig. 2B). This Vector Summation Model is not related to the specific geometry of the limb during the task. Rather, this model supposes that brain activity can be represented by a coordinate frame of the motor periphery with each mechanical degree-of-freedom (DOF) representing an independent, orthogonal axis. When loads are applied at both the shoulder and elbow, the estimated activity of the cell equals the vector summation of the cell's response when loads are applied independently at the shoulder (Vector S) and elbow (Vector E). The predicted activity of each cell was computed for each model and compared with the actual discharge rate of the cell for the multi-joint loads (the length of Vector ES).

Electromyographic (EMG) activity of proximal arm muscles was recorded using pairs of single-strand wires inserted percutaneously in three monkeys, as well as through pairs of multi-strand wires implanted chronically in the first monkey under aseptic conditions (see Loeb and Gans 1986; Scott and Kalaska 1997). Most muscles spanning the shoulder and elbow joints were sampled in at least one of the three monkeys including mono-articular (anterior, posterior, and middle deltoids, pectoralis major, brachialis, brachioradialis, infraspinatus, supraspinatus, teres major, subscapularis and latissimus dorsi, medial, lateral triceps) and bi-articular muscles that span both joints (long head of triceps, dorso-epitrochlearis, long and short head of biceps). Some muscles in the first monkey were sampled twice, once with percutanous electrodes and once with chronic electrodes. Although electrode placement was usually obvious due to the minimal adipose tissue overlying the forelimb muscles, the location of the wires was assessed using microstimulation through the recording leads (<2 mA, 33 Hz for 333 ms). The techniques described above to interpret neural activity (directional tuning and significant modulation with joint loads) were also used to interpret the activity of the proximal limb muscles based on the integrated electromyographic activity during the last 2 s of each trial.

RESULTS

We recorded the activity of 160 neurons in the proximal-arm region of MI. Of these neurons, 107 modulated their activity for mechanical loads at the shoulder or elbow (ANOVA, $P <$

0.01) and were analyzed further to examine how their discharge was related to torque at the two joints. The activity of 74 and 68 neurons showed a significant change in activity when loads were applied to the shoulder and elbow, respectively (ANOVA, $P < 0.01$). Most of these cells showed a reciprocal change in activity with torque where roughly equal numbers of neurons increased activity for flexor or extensor torque and decreased activity for the other. Across the population, cell activity was equally responsive to shoulder and elbow loads (average difference between flexor and extensor shoulder loads, 11.9 ± 7.9 spikes/s, mean $\pm$ SD; elbow loads, 10.8 ± 8.2 spikes/s).

We found that some cells modulated their activity when the monkey compensated for mechanical loads applied at only one joint, but were unresponsive to loads applied at the other joint. Figure 1B illustrates a neuron that modulated its activity with changes in muscular torque at the shoulder, but did not show any significant modulation with changes in torque at the elbow (ANOVA, $P < 0.01$). The diagram on the right illustrates activity for this cell as a contour plot in joint-torque space. A high discharge rate is colored red, and a low discharge rate is blue. The near vertical banding pattern of colors illustrates that this neuron modulated its activity with loads at the shoulder (horizontal axis) and was insensitive to loads at the elbow (vertical axis). The black arrow, the preferred direction of the

cell in joint-torque space, is oriented to the right aligned with the shoulder flexor axis (PD = 2°, $P < 0.01$). A total of 39 cells modulated their activity only for loads applied to the shoulder, whereas 33 cells were sensitive to loads only at the elbow (ANOVA, $P < 0.01$).

We also found that 35 neurons were sensitive to mechanical loads applied at both joints (ANOVA, $P < 0.01$). Figure 1C illustrates the activity of a cell for the nine load conditions. Neural activity tended to increase for shoulder extensor and elbow flexor loads. Maximal activity was observed when the monkey generated a shoulder extensor torque combined with an elbow flexor torque. The preferred direction of this cell in joint-torque space was oriented diagonally in the top left quadrant (PD = 138°, black arrow in *right panel* of Fig. 1C).

The present observations illustrate that MI cells can covary their discharge with mechanical loads at more than one joint, and raise the important question of how the activity of MI cells reflects motor patterns at multiple joints simultaneously. Across the population of neurons, the Linear Summation Model tended to overestimate the discharge pattern of cells (Fig. 2A; paired *t*-test, $n = 107$, $P < 10^{-10}$). To ensure that the overestimation of the linear summation model was not simply due to clipping at low discharge rates or due to saturation at high discharge rates during certain loads, we reexamined the response of a subset of primary motor cortical neurons that
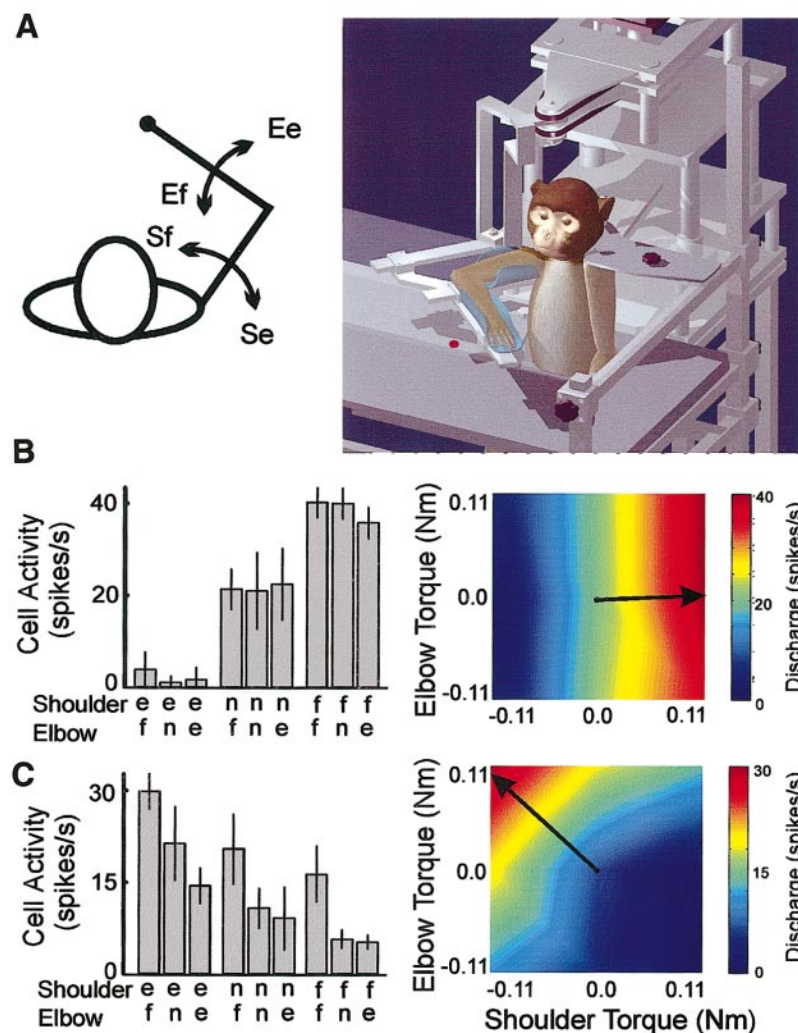

FIG. 1. *A*: on the right is a computer-generated illustration of a monkey and the mechanical device used to monitor and manipulate the mechanics of the shoulder and elbow joints during planar arm motor tasks. The diagram on the *left* shows the sign convention for flexors and extensors at each joint. S and E, shoulder and elbow joints, respectively; f and e, flexor and extensor muscle groups, respectively. *B*: on the *left,* variations in cell discharge rate for a motor cortical cell relative to muscular torque at the shoulder and elbow joints. Bar height denotes the mean, and the black lines denote SD for 5 repeat trials. Cell discharge rate varied strongly with shoulder muscular torque but was not responsive to changes in elbow muscular torque. e, n, and f denote extensor, no-load, and flexor conditions, respectively, at the shoulder and elbow. On the *right* is the discharge of the same cell as a contour map in a joint-based coordinate frame with positive axes signifying flexor muscular torque at the shoulder and elbow (*x*- and *y*-axes, respectively). The black arrow defines the cell's preferred direction in joint-torque space. The orientation of the arrow along the positive horizontal axis signifies that this cell was maximally active when the monkey generated a shoulder flexor torque. *C*: the activity of a neuron with a complex relationship to muscular torque at the shoulder and elbow joints. Neural activity tended to increase when the monkey generated shoulder extensor or elbow flexor muscular torque and was maximally active when generating this combination of torques at the 2 joints.
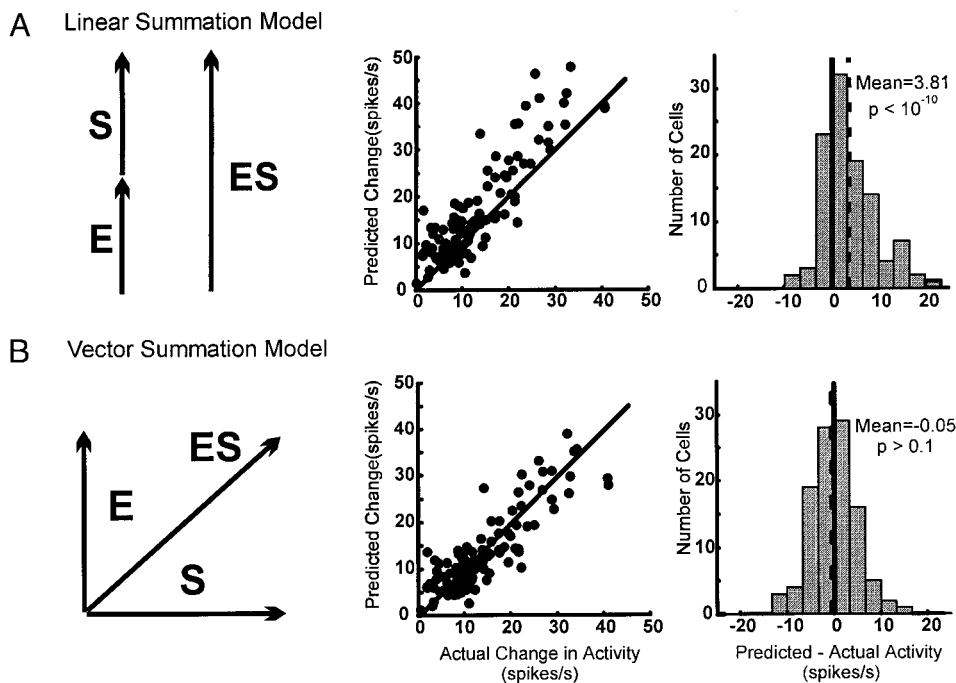
FIG. 2. Prediction of the discharge pattern of motor cortical cells for multi-joint loads. *A*: plot at *left* illustrates how neural activity during multi-joint loads (Vector ES) is predicted as the simple addition of its activity when only the elbow (Vector E) or the shoulder (Vector S) are loaded (Linear Summation Model, see text). The *middle plot* compares the actual vs. predicted changes in discharge for multi-joint loads using this model. The line ($y = x$) represents a perfect match between the predicted and actual discharge rate. Note that most points fall above this line so that the predicted change in cell discharge tended to overestimate the observed change in discharge. The histogram on the *right* also illustrates the systematic overprediction of cell discharge for the linear summation model (mean difference = 3.81 spikes/s; $P < 10^{-10}$). *B*: plot at *left* illustrates how neural activity during multi-joint loads (Vector ES) is predicted as the vector summation of its activity when only the elbow (Vector E) or only the shoulder (Vector S) are loaded (Vector Summation Model, see text). *Middle panel* compares the actual vs. predicted changes in discharge for multi-joint loads. Data points are distributed equally above and below the unity line. The histogram to the *right* illustrates that the difference between predicted and actual activity is centered around zero (mean difference = -0.05 spikes/s; $P > 0.10$).

fulfilled two criteria. First, cell discharge rate had to remain above 5 spikes/s for all load conditions. Second, cell activity also had to be recorded during a reaching task, and the maximal discharge during the postural task had to be at least 20% less than peak discharge rate during movement. This latter criterion was used to demonstrate that the discharge rate of the cell had not saturated during the postural task. Even with these strict criteria, the Linear Summation Model still over-predicted the discharge rate of this subpopulation of cells ($n = 36$, paired t-test, $P < 10^{-5}$). The failure of the linear summation model suggests that motor cortical cells reflect a more complex signal related to the two joints. In general, estimates of neural activity when loads were applied to both joints based on neural activity when loads were applied to each joint independently were much better when using the Vector Summation Model. Across the population, this model could predict the activity of motor cortical cells for combined loads at the shoulder and elbow joints (Fig. 2*B*; paired t-test, $n = 107$, $P > 0.10$).

One of the most interesting observations we found was that there was a specialized organization for representing mechanical loads applied at the two joints. Most multi-joint neurons (30/35, 86%) were maximally active for mechanical loads that required flexor muscular torque at one joint combined with extensor muscular torque at the other, or vice versa. Significantly fewer neurons (5/35, 14%) were maximally active when either flexor or extensor torques were generated at both joints ($P < 0.01$, χ^2 test against equal probabilities for each group).

This overrepresentation of flexor torque at one joint combined with extensor at the other can be illustrated by plotting the distribution of PDs of MI cells in joint-torque space (Fig. 3). Eighty-eight cells were directionally tuned to the load
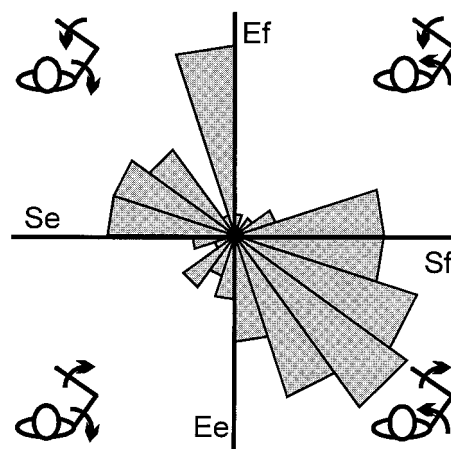

FIG. 3. Distribution of preferred directions in joint-torque space ($n = 88$). The size of each pie slice is proportional to the number of cells with preferred directions in each 18° sector. The four icons represent the joint muscular torque represented in each quadrant. We found that the distribution of PDs was not uniform (Rayleigh test against a bimodal distribution, $P < 0.001$). Rather, there were 2 clusters in the distribution, one related to shoulder flexor and elbow extensor muscular torques and one related to shoulder extensor and elbow flexor torques.

according to the bootstrap test. The size of each pie slice is proportional to the number of cells maximally active for a given combination of loads at the two joints. The distribution is statistically nonuniform with two clear clusters, one related to elbow flexors and shoulder extensors and another cluster associated with elbow extensors and shoulder flexors ($P <$ 0.001, Bimodal Rayleigh test) (Batschelet 1981). The major axis of the distribution was 143–323° (angle defined counterclockwise from x-axis). This asymmetry cannot be explained by the action of biarticular muscles since biarticular biceps and triceps muscles provide combined flexor or combined extensor muscle torques, respectively (*top right* and *bottom left* quadrants in Fig. 3).

Electromyographic activity was recorded in a total of 48 muscles during the task, and 41 of these were found to be modulated by loads at the shoulder or elbow (ANOVA, $P <$ 0.01). The activity of a majority of muscles (25/41) was sensitive to loads at both joints, with fewer responsive only to loads at the shoulder (7) or elbow (9). This is somewhat surprising since only seven of the muscles in our sample from the three monkeys spanned both joints (biarticular muscles). The activity of 19 of 34 monoarticular muscles were responsive to loads applied at both joints. Figure 4, *A* and *B,* illustrates variations in the activity of two monoarticular muscles for the nine load conditions. The activity of anterior deltoid, a shoulder flexor, was only dependent on the net muscular torque at the shoulder (ANOVA, $P > 0.01$; Fig. 4A). In contrast, the activity of brachioradialis, an elbow flexor, increased when the monkey generated an elbow flexor torque and was most active when the monkey also generated a shoulder extensor torque as compared with a shoulder flexor torque. The response of specific muscles was generally similar across the three monkeys.

A total of 34 muscles was defined as directionally tuned in joint-torque space ($P < 0.01$). The directional preference of 27 (79%) of these muscles was maximally active for loads that required flexor torque at one joint combined with extensor torque at the other, or vice versa ($P < 0.01$, χ^2 test against equal probabilities for each group). Figure 4C illustrates the distribution of PDs for the activity of forelimb muscles sampled in this study. The distribution was not uniform when compared against a unimodal distribution (115°, $z = 5.51$, $P <$ 0.01, Unimodal Rayleigh test), but this nonuniformity was even more pronounced when tested against a bimodal distribution (128–308° for major axis, $z = 9.95$, $P < 0.001$, Bimodal Rayleigh test).

DISCUSSION

It seems intuitive that the activity of a single-joint muscle would simply reflect the mechanical load at the spanned joint. However, we found that the activity of many single-joint muscles was dependent on the load applied at both the spanned and nonspanned joints. Similar couplings have been observed for muscles during elbow flexion/extension and supination/pronation in humans (Buchanon et al. 1989; van Zuylen et al. 1988), as well as for individuated finger movements in nonhuman primates (Schieber 1995). This coupling is not related to intersegmental dynamics since there is no body motion in our postural task. Rather, this coupling can be best understood as a consequence of the mechanical action of biarticular muscles. Any activity in these muscles to oppose a mechanical load at one joint creates muscular torque at the other joint, which must then be opposed by corresponding antagonistic muscle activity at this other joint. For example, activity in biceps to generate an
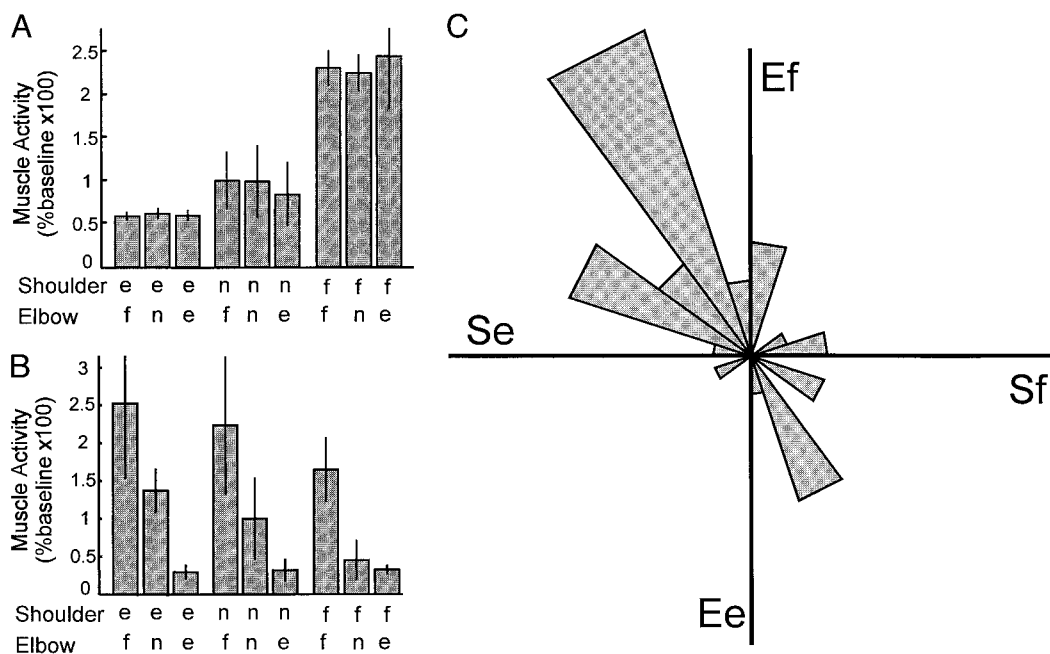

FIG. 4. *A*: variations in electromyograph (EMG) of anterior deltoid, a shoulder flexor, when the monkey compensated for mechanical loads at the shoulder and elbow joints (mean ± SD). Muscle activity varied strongly with shoulder muscular torque and was not responsive to changes in elbow muscular torque. e, n, and f denote extensor, no-load, and flexor conditions, respectively, at the shoulder and elbow. *B*: variations in EMG of brachioradialis, an elbow flexor, for the 9 load conditions. Activity tended to increase when the monkey generated elbow flexor or shoulder extensor muscular torque and was maximally active when generating this combination of torques. *C*: distribution of preferred directions in joint-torque space based on the activity of shoulder and elbow muscles recorded during the task ($n = 34$).

elbow flexor torque to oppose a load also creates a flexor torque at the shoulder that is compensated by recruitment of shoulder extensor muscles. Such coupling complicates the mapping between joint torque and muscle activity and obfuscates attempts to delineate and dissociate motor patterns based on experimentally defined degrees-of-freedom of the limb. More importantly, the action of biarticular muscles provides many advantages to the motor system such as improved coordination (Zajac 1993), energy transfer (Bobbert and van Ingen Schenau 1988), and stabilization (McIntyre et al. 1996; Osu and Gomi 1999).

We found that roughly equal numbers of neurons were statistically related to loads only at the shoulder, loads only at the elbow and loads at both joints. This latter group of multi-joint cells would appear to demonstrate that single neurons are involved in controlling motor patterns at multiple joints, a physiological correlate of corticomotoneurons that synapse on motoneurons of muscles at both the shoulder and elbow (McKiernan et al. 1998). However, as stated above, since the activity of some monoarticular muscles was modulated by loads applied at both the shoulder and elbow, we cannot conclude at this time that "multi-joint" neurons are necessarily involved in the control of multiple muscles spanning different joints.

The present goal-directed motor task can be interpreted using the coordinate transformation model where the CNS performs a series of sensorimotor transformations from a signal of spatial location to a pattern of muscle activity including intermediary representations related to hand and joints (Kalaska et al. 1997; Soechting and Flanders 1992). The present postural task specifically addresses the later representations since the spatial target, hand, and joint kinematics all remained constant while joint torque and muscle activation patterns were varied. We directly manipulated joint torque in this task so that all combinations of torque at the two joints were equally tested. Yet, the distribution of PDs of MI neurons was not uniform in joint-torque space, but was skewed toward one of two quadrants and suggests that the load-related activity in MI is not a simple representation of joint torque. The distribution of PDs of shoulder and elbow muscle activities showed a similar skew suggesting that MI activity during this task at least partially reflects the selection of muscle activities for the task. If MI does not explicitly represent joint torque, then it is difficult to identify where such a representation would exist since most other cortical regions involved in these volitional limb motor tasks, such as dorsal premotor cortex or parietal area 5, tend to be less sensitive to variables related to the limb, such as arm geometry or load (Kalaska et al. 1989; Scott et al. 1997). One remaining possibility is cerebellum since neural activity in dentate and interpositus nuclei have been shown to be sensitive to mechanical loads (Thach 1978).

However, our observation that cell activities during multi-joint loads are best predicted by the Vector Summation Model does illustrate the heuristic value of interpreting neuronal activities in MI in joint-based frames, such as joint torque. One could conceive of a large variety of ways in which a cell could respond to single- and multi-joint loads. In general, suppose that you plot the response of a cell to a given pattern of loads as a vector in some arbitrary coordinate space, where the length of the vector is proportional to cell discharge and the direction represents the pattern of the loads. Thus a load at only the elbow might be represented by one vector while a load at only the shoulder might be represented by another, and a load at both joints simultaneously might be represented by still another vector. Is there a simple way in which these vectors might be related? Both the Linear and the Vector model are really special cases of a general model that assumes that responses to multi-joint loads are a sum of the vector responses to single-joint loads. The difference lies in how the single-joint vectors are oriented with respect to each other; in the Linear Model they are collinear, in the Vector Model they are orthogonal. In general, given an arbitrary relationship between cell activity and load pattern, one cannot expect any particular angle between single-load responses to yield a sum vector that predicts the multi-load response. The fact that orthogonal vectors make the best prediction implies that MI cells use a particular special case where MI cell activity related to the shoulder and elbow joints can be treated as independent axes. One might therefore suggest that in more complex movements, other DOFs that come into play would define still other orthogonal axes in the coordinate system used to control posture, an empirical prediction that could be tested in experiments with three-dimensional or redundant-DOF planar movements. It is important to note that the success of the Vector Summation Model was based on the neural responses across the sampled population of cells. Future work will examine whether the activity of individual neurons fit with the Vector or Linear Summation Models or other more arbitrary representations.

REFERENCES

Batschelet E. *Mathematics in Biology: Circular Statistics in Biology.* London: Academic, 1981.

Bobbert MF and van Ingen Schenau GJ. Coordination in vertical jumping. *J Biomechanics* 21: 249–262, 1988.

Buchanan TS, Rovai GP, and Rymer WZ. Strategies for muscle activation during isometric torque generation at the human elbow. *J Neurophysiol* 62: 1201–1212, 1989.

Cisek P and Scott SH. Cooperative action of mono- and bi-articular arm muscles during multi-joint posture and movement tasks in monkeys. *27th Meet Soc Neurosci* 24: 164.4, 1998.

Drew T, Jiang W, Kably B, and Lavoie S. Role of motor cortex in the control of visually triggered gait modifications. *Can J Physiol Pharmacol* 74: 426–442, 1996.

Georgopoulos AP. Current issues in directional motor control. *Trends Neurosci* 18: 506–510, 1995.

Georgopoulos AP, Kalaska JF, Caminiti R, and Massey JT. On the relations between the direction of two-dimensional arm movements and cell discharge in primate motor cortex. *J Neurosci* 2: 1527–1537, 1982.

Kakei S, Hoffman DS, and Strick PL. Muscle and movement representations in the primary motor cortex. *Science* 285: 2136–2139, 1999.

Kalaska JF, Cohen DA, Hyde ML, and Prud'homme M. A comparison of movement direction-related versus load direction-related activity in primate motor cortex, using a two-dimensional reaching task. *J Neurosci* 9: 2080–2102, 1989.

Kalaska JF, Scott SH, Cisek P, and Sergio LE. Cortical control of reaching movements. *Curr Opin Neurobiol* 7: 849–859, 1997.

Loeb GE and Gans C. *Electromyography for Experimentalists.* Chicago, IL: Univ. of Chicago Press, 1986.

MCINTYRE J, MUSSA-IVALDI FA, AND BIZZI E. The control of stable postures in the multijoint arm. *Exp Brain Res* 110: 248–264, 1996.

MCKIERNAN BJ, MARCARIO K, KARRER JH, AND CHENEY PD. Corticomotoneuronal postspike effects in shoulder, elbow, wrist, digit, and intrinsic hand muscles during a reach and prehension task. *J Neurophysiol* 80: 1961–1980, 1998.

MURPHY JT, WONG YC, AND KWAN HC. Sequential activation of neurons in primate motor cortex during unrestrained forelimb movement. *J Neurophysiol* 53: 435–445, 1985.

OSU R AND GOMI H. Multijoint muscle regulation mechanisms examined by measured human arm stiffness and EMG signals. *J Neurophysiol* 81: 1458–1468, 1999.

SCHIEBER MH. Muscular production of individuated finger movements: the roles of extrinsic finger muscles. *J Neurosci* 15: 284–297, 1995.

SCOTT SH. Apparatus for measuring and perturbing shoulder and elbow joint positions and torques during reaching. *J Neurosci Methods* 89: 119–127, 1999.

SCOTT SH. Role of motor cortex in coordinating multi-joint movements: is it time for a new paradigm? *Can J Physiol Pharmacol* 78: 923–933, 2000.

SCOTT SH AND KALASKA JF. Reaching movements with similar hand paths but different arm orientations. I. Activity of individual cells in motor cortex. *J Neurophysiol* 77: 826–852, 1997.

SCOTT SH, SERGIO LE, AND KALASKA JF. Reaching movements with similar hand paths but different arm orientations. II. Activity of individual cells in dorsal premotor cortex and parietal area 5. *J Neurophysiol* 78: 2413–2426, 1997.

SOECHTING JF AND FLANDERS M. Moving in three-dimensional space: frames of reference, vectors, and coordinate systems. *Annu Rev Neurosci* 15: 167–191, 1992.

THACH WT. Correlation of neural discharge with pattern and force of muscular activity, joint position, and direction of intended next movement in motor cortex and cerebellum. *J Neurophysiol* 41: 654–676, 1978.

VAN ZUYLEN EJ, GIELEN CCAM, AND DENIER VAN DER GON JJ. Coordination and inhomogeneous activation of human arm muscles during isometric torques. *J Neurophysiol* 60: 1523–1548, 1988.

ZAJAC FE. Muscle coordination of movement: a perspective. *J Biomechanics* 26: 2109–2124, 1993.